

Al solubility in ZnO nanocrystals synthesized by solvothermal method

XIAOJIE YANG¹, YUQI LIU², YECHENG PEI², DONGYUN GUO^{2,*}

¹Faculty of Building Materials, Kunming Metallurgy College, 650033, China

²School of Materials Science and Engineering, Wuhan University of Technology, 430070, China

The Al-doped ZnO nanocrystals were synthesized by a solvothermal method with nominal Al content ranging from 3 to 7 at.% in the precursors, and the Al solubility in ZnO nanocrystals was investigated. When the nominal Al content in the precursors was less than 5 at.%, the single-phase Al-doped ZnO nanocrystals with wurtzite structure were synthesized at 260 °C for 20 h. The maximum Al solubility in ZnO nanocrystals was about 2.97 at.%, as the the nominal Al content in the precursor was 5 at.%. In the solvothermal process, the Al-doped ZnO nanocrystals tended to grow along the *c*-axis direction to form nanorods based on the oriented-attachment growth mechanism.

(Received December 14, 2021; accepted June 6, 2022)

Keywords: Al-doped ZnO nanocrystals, Solvothermal method, Al solubility, Oriented attachment

1. Introduction

Transparent conductive oxides are characterized by a combination of high electrical conductivity, and high transparency in the visible and near infrared spectral range, which are widely applied in optoelectronic devices and photovoltaic devices [1-3]. Indium tin oxide (ITO) is a typical transparent conductive oxide with good optoelectronic properties. However, the scarcity of indium hampers the extended application of ITO transparent electrode. Al-doped ZnO has been widely studied as a potential alternative to the expensive ITO transparent electrode, due to the abundance of Al and Zn elements in the nature and non-toxicity [4, 5]. Since ZnO compound is a semiconductor with wide direct band gap energy of 3.3 eV, Al doping plays an important role in increasing its electrical conductivity. It is very difficult to substitute Zn²⁺ ions by Al³⁺ ions due to the difference in oxidation state, ionic radius and coordination preference [6].

In recent years, many researchers investigated the solubility limit of Al³⁺ ions in ZnO. Serier et al. [6] synthesized Al-doped ZnO powders at 850 °C for 10 h under air by a Pechini route with a doping rate varying from 1 to 4 at.%, and the Al solubility limit was estimated under 0.3 at.%. Zhang et al. [7] prepared Al-doped ZnO nanopowders by a sol-gel method. The Al solubility was determined to be 0.9 at.%, and the ZnAl₂O₄ was formed once the Al content achieved 1.0 at.% or above. Damm et al. [8] synthesized Al-doped ZnO nanoparticles by a thermal decomposition method, and they demonstrated the incorporation of Al³⁺ ions inside the ZnO crystal lattice and interstitial Al³⁺ substitution. However, they didn't report the definite Al³⁺ doping content in the ZnO crystal

lattice. Giovannelli et al. [9] synthesized Al-doped ZnO nanoparticles by an aqueous coprecipitation, and the Al content in the ZnO nanoparticles didn't exceed 0.3 at.%. Cornelius et al. [10] investigated Al³⁺ doping in ZnO thin films grown by a pulsed reactive magnetron sputtering, and the resistivity minimum was obtained as the Al content was 1.7 at.%. The metastable Al super-saturated solid solution tended to segregate into ZnO and ZnAl₂O₄ spinel when growth conditions approached thermodynamic equilibrium. They found that the increase of Al content in the sputtering target resulted in an increase of structural disorder which manifested in buildup of microscopic strain, loss of *c*-axis texture and an increased density of grain-boundary related defects. Wu et al. [11] investigated Al-doping distribution in atomic layer deposited ZnO thin films. An enrichment of the Al³⁺ ions at grain boundaries was observed, and the low doping efficiency for local Al densities was ascribed to the Al solubility limit in ZnO and to the suppression of the ionization of Al dopants from adjacent Al donors. Recently, Mukherjee et al. [12] reported Al-doped ZnO nanoparticles with high Al content (6 at.%) synthesized by a simple chemical route at low temperature. However, in our previous study, as the Al-doped ZnO thin films were prepared by the similar chemical route, the substitution of Al³⁺ ions for Zn²⁺ ions was quite difficult in the ZnO crystal lattice, and the Al³⁺ ions mainly accumulated at the grain boundaries [13]. When the Al-doped ZnO nanocrystals were synthesized by a solvothermal method at 160 °C for 30 min, the Al content in the nanocrystals was about 2.7 at.%, [14] which was much higher than the Al solubility limit reported by Serier et al. [6]. This result indicated that the high pressure in the autoclave could

improve the Al doping coefficient. According these research results, it is necessary to further investigate the Al-doping in ZnO nanocrystals synthesized by the solvothermal method. In this study, the Al-doped ZnO nanocrystals were synthesized by the solvothermal method at high reaction temperature, and the Al solubility limit was investigated.

2. Experimental details

All the reagents were of analytical grade purity and were used without further purification. Zinc acetate dihydrate ($\text{Zn}(\text{CH}_3\text{COO})_2 \cdot 2\text{H}_2\text{O}$) and aluminum diacetate hydroxide ($\text{Al}(\text{OH})(\text{COOCH}_3)_2$) were used as the starting materials. The desired amounts of $\text{Zn}(\text{CH}_3\text{COO})_2 \cdot 2\text{H}_2\text{O}$ and $\text{Al}(\text{OH})(\text{COOCH}_3)_2$ were dissolved in 30 ml methanol at room temperature with stirring to form the transparent precursors, and the concentration was 0.2 mol/L. The nominal Al content was calculated by the atomic ratio of $\text{Al}/(\text{Zn}+\text{Al})$ in the precursors. In this study, the nominal Al contents were 3, 5 and 7 at.%, respectively. The 30 ml precursors were added to Teflon-lined autoclaves of 50 ml capacity. The autoclaves were sealed tightly, and heated at 260 °C for 20 h with stirring. Finally, they were naturally cooled to room temperature. The precipitates were washed with deionized water and ethanol in sequence.

The crystal phase of the precipitates was analyzed by an X-ray diffractometer (XRD, D/MAX-RB) with $\text{CuK}\alpha$ radiation (40 kV, 30 mA) with scanning rate of 2 °/min and scanning step of 0.02°. Their morphologies were characterized by a high-resolution transmission electron microscopy (TEM, JEM-2100F), and energy-dispersive spectra (EDS) were examined with an EDS detector working at an accelerating voltage of 30 kV.

3. Results and discussions

Fig. 1 shows the XRD results of precipitates with different nominal Al contents in the precursors. The XRD patterns were indexed according to JCPDS 36-1451 (hexagonal ZnO phase with space group P63mc). All precipitates showed the clear and sharp diffraction peaks of hexagonal ZnO phase, which indicated that ZnO phase with wurtzite structure was formed. As the nominal Al content increased from 3 to 5 at.%, the intensity of diffraction peaks obviously decreased. When the nominal Al content increased to 7 at.%, the second phase of $\text{Zn}_6\text{Al}_2(\text{OH})_{16}\text{CO}_3 \cdot 4\text{H}_2\text{O}$ was observed.

Fig. 2 displays the morphologies of Al-doped ZnO

precipitates with different nominal Al contents in the precursors. The quasi-spherical nanoparticles were formed, and the grain size ranged from 10 to 20 nm. The aggregated quasi-spherical nanoparticles tended to form the short rods with pearl-chain-like structures, as depicted by Pacholski et al. [15]. The Al contents in the Al-doped ZnO precipitates were characterized by the EDS technique, and the results are listed in Table 1. Nasr et al. [16] prepared Al-doped ZnO thin films by sol-gel method with nominal Al doping (0-4 at.%), and the Al solubility limit was about 2 at.%. They indicated that the Al solubility in nanocrystalline materials increased compared to the bulk solubility. In our previous study, the Al-doped ZnO nanocrystals were synthesized by the solvothermal method, and the maximum Al solubility was about 2.7 at.% [14]. In this study, as the nominal Al content in the precursor was 5 at.%, the Al content in the Al-doped ZnO nanocrystals was 2.97 at.%. The Al doping content increased, which might be attributed to the higher reaction temperature.

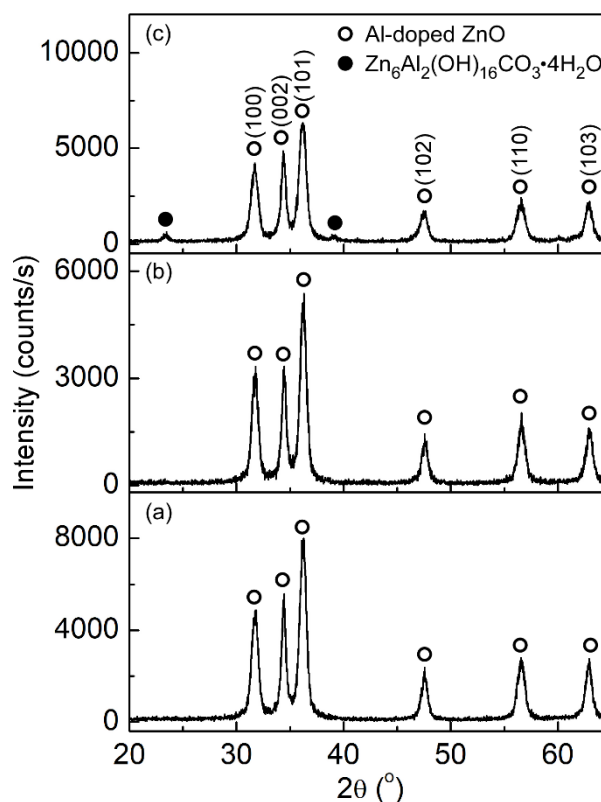


Fig. 1. XRD patterns of Al-doped ZnO nanocrystals with different nominal Al contents in the precursors: (a) 3 at.%, (b) 5 at.% and (c) 7 at.%

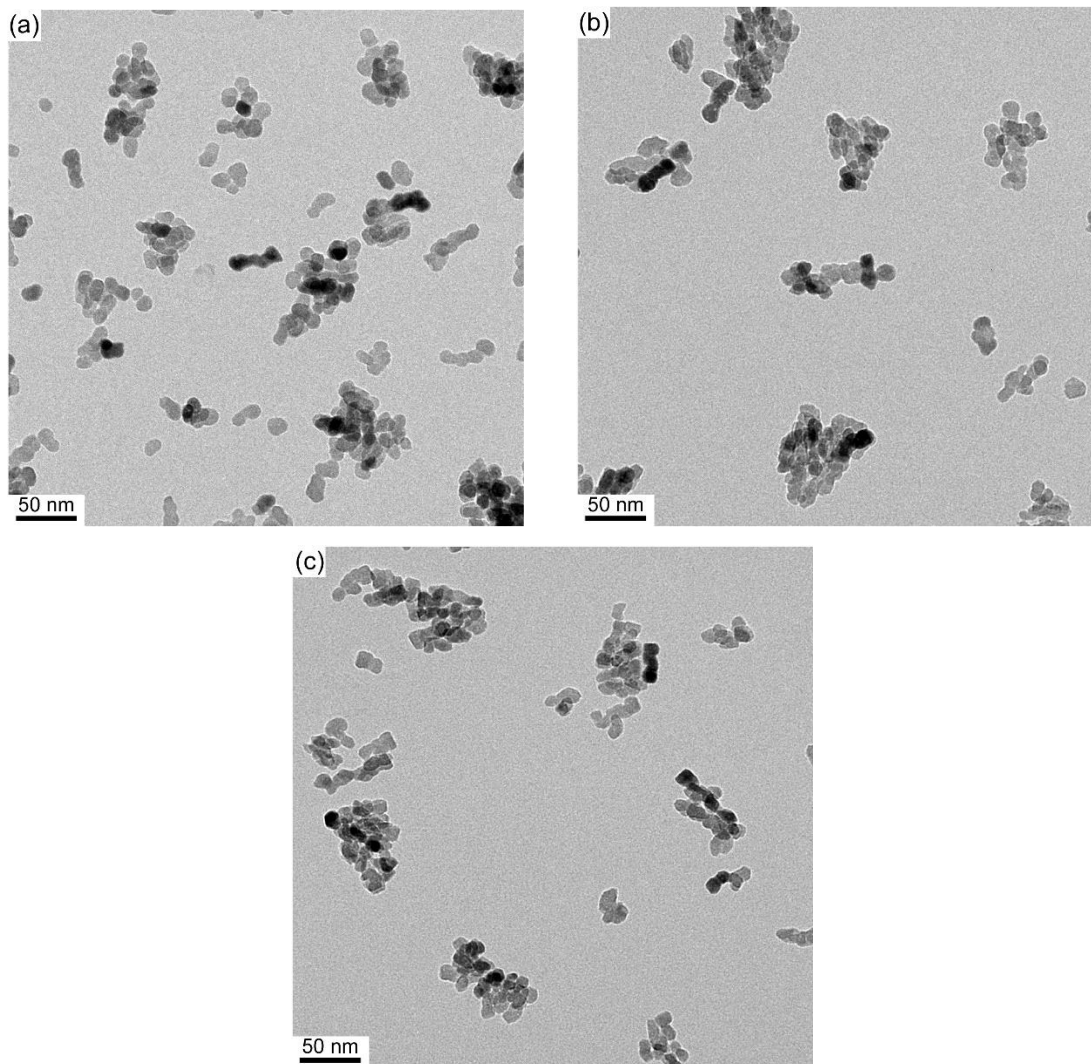


Fig. 2. Morphologies of Al-doped ZnO nanocrystals with different nominal Al contents in the precursors: (a) 3 at.%, (b) 5 at.% and (c) 7 at.%

Table 1. Al content in the Al-doped ZnO precipitates according to EDS analysis

| Sample | Nominal Al content (at.%) | Al content (at.%) |
|--------|---------------------------|-------------------|
| 1 | 3 | 1.95 |
| 2 | 5 | 2.97 |
| 3 | 7 | 5.10 |

The detailed TEM investigations of the Al-doped ZnO nanocrystals with nominal Al content of 3 at.% was done to analyze the growth mechanism. At low magnification,

the short rods with pearl-chain-like structure were observed, as shown in Fig. 3(a). The high-resolution TEM images of a series of aggregated nanocrystals are shown in Figs. 3(b, c and d). The lattice planes of the aggregated nanocrystals were almost perfectly aligned, and the Al-doped ZnO nanocrystals were epitaxially fused together. The bottlenecks between the adjacent nanocrystals were visible, and the observed lattice planes in these images were (002), which indicated that the Al-doped ZnO nanocrystals tended to grow along the *c*-axis direction based on the oriented attachment [17, 18].

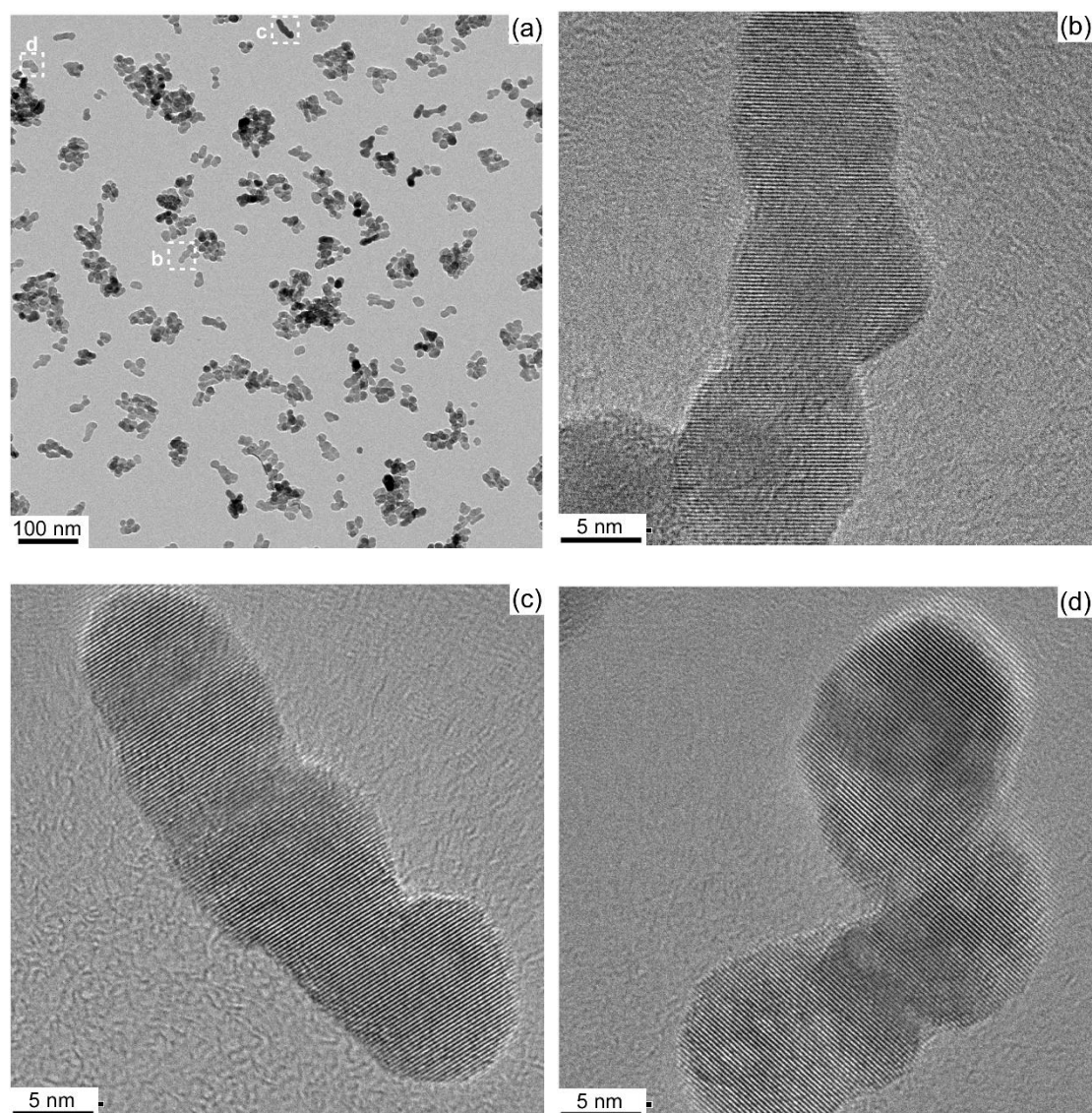


Fig. 3. TEM images of Al-doped ZnO nanocrystals with the nominal Al content of 3 at.% in the precursor

4. Conclusions

The Al-doped ZnO nanocrystals were synthesized by the solvothermal method. The single-phase Al-doped ZnO nanocrystals with wurtzite structure were obtained at 260 °C for 20 h, as the nominal Al content in the precursors was less than 5 at.%. The Al solubility limit was about 2.97 at.% at the nominal Al content of 5 at.% in the precursor. The Al-doped ZnO nanocrystals tended to grow along the *c*-axis direction to form the nanorods based on the oriented-attachment growth mechanism.

Acknowledgements

This work was supported by the National Natural Science Foundation of China (Grant No. 50902108).

References

- [1] Q. Zheng, Z. Li, J. Yang, J. Kim, *Prog. Mater. Sci.* **64**, 200 (2014).
- [2] O. Edynoor, A. R. M. Warikh, T. Moriga, K. Murai, M. E. A. Manaf, *Rev. Adv. Mater. Sci.* **49**, 150 (2017).
- [3] Y. Fang, D. Commandeur, W. C. Lee, Q. Chen, *Nanoscale Adv.* **2**, 626 (2020).
- [4] R. Yan, T. Takahashi, H. Zeng, T. Hosomi, M. Kanai, G. Zhang, K. Nagashima, T. Yanagida, *ACS Appl. Electron. Mater.* **3**, 955 (2021).
- [5] J. H. Kwon, Y. Jeon, K. C. Choi, *ACS Appl. Mater. Interfaces* **10**, 32387 (2018).
- [6] H. Serier, M. Gaudon, M. Menetrier, *Solid State Sci.* **11**, 1192 (2009).
- [7] Y. Zhang, W. Wang, R. Tan, Y. Yang, X. Zhang, P. Cui, W. Song, *Int. J. Appl. Ceram. Technol.* **9**, 374

- (2012).
- [8] H. Damm, A. Kelchtermans, A. Bertha, F. V. den Broeck, K. Elen, J. C. Martins, R. Carleer, J. D'Haen, C. De Dobbelaere, J. Hadermann, A. Hardy, M. K. Van Bael, *RSC Adv.* **3**, 23745 (2013).
- [9] F. Giovannelli, A. Ngo Ndimba, P. Diaz-Chao, M. Motelica-Heino, P. I. Raynal, C. Autret, F. Delorme, *Powder Technol.* **262**, 203 (2014).
- [10] S. Cornelius, M. Vinnichenko, *Thin Solid Films* **605**, 20 (2016).
- [11] Y. Wu, A. Devin Giddings, M. A. Verheijen, B. Macco, T. J. Prosa, D. J. Larson, F. Roozeboom, W. M. M. Kessels, *Chem. Mater.* **30**, 1209 (2018).
- [12] S. Mukherjee, S. Pramanik, S. Das, S. Chakraborty, R. Nath, P. K. Kuri, *J. Alloys Comp.* **814**, 152015 (2020).
- [13] D. Guo, L. Liu, X. Li, Z. Huang, L. Zhang, K. Kato, *J. Optoelectron. Adv. M.* **22**, 75 (2020).
- [14] D. Guo, K. Sato, S. Hibino, T. Takeuchi, H. Bessho, K. Kato, *J. Mater. Sci.* **49**, 4722 (2014).
- [15] C. Pacholski, A. Kornowski, H. Weller, *Angew. Chem. Int. Ed.* **41**, 1188 (2002).
- [16] B. Nasr, S. Dasgupta, D. Wang, N. Mechau, R. Kruk, H. Hahn, *J. Appl. Phys.* **108**, 103721 (2010).
- [17] F. Huang, H. Zhang, J. F. Banfield, *Nano Lett.* **3**, 373 (2003).
- [18] D. Li, M. H. Nielsen, J. R. I. Lee, C. Frandsen, J. F. Banfield, *J. J. De Yoreo, Science* **336**, 1014 (2012).

*Corresponding author: guody@whut.edu.cn